Design and Performance of a Thin, Solid Layer for High-Resolution, Dry-Contact Acoustic Imaging

Hironori Tohmyoh and Masumi Saka

***Abstract*—Compared to the usual water immersion case, more effective transmission and reception of high-frequency ultrasound through a thin, solid layer are reported. A theoretical model is presented to perform the signal amplification and the signal modulation toward the higher frequency components for getting the high-quality acoustic images without immersing the object to be imaged. Also, the thin, solid layers are designed from the theoretical model, and the transmission of high-frequency ultrasound is carried out through the layer/silicon interfaces with an applied pressure of about 0.1 MPa. The spectral intensity in the frequency range of 20 to 70 MHz remarkably improves compared with water immersion, and the peak frequencies of the spectra modulate the higher than water immersion. Furthermore, the solder joint inspection of a package is performed. The present dry-contact technique achieves the higher spatial resolution and the higher signal-to-noise ratio (SNR) than the usual water immersion technique, and clearly detects the defective joint without getting the package wet.**

I. Introduction

Acoustic microscopy is widely used for high-resolution imaging and nondestructive evaluation in many areas, especially in the electronics industry for the visualization of bonding, delamination, and cracks in semiconductor devices [1]. It also is used in the spacecraft industry for the detection of cracks, delaminations, and broken fibers in composite materials [2]. Commonly, this has to be performed by immersing the tested parts in coupling liquid for transmitting the ultrasound into the tested parts. Usually, water is used as the coupling liquid [3]; but in many situations, this is undesirable as devices and materials may become contaminated through water/moisture absorption. For example, the moisture absorption in semiconductor devices causes the generation of delamination and cracks in the devices [4], and the moisture absorption in composite materials also may affect adversatively the strength [5].

To overcome the inherent problems of the usual immersion technique, several attempts have been made on the transmission and reception of ultrasound without liquid immersion. One of these techniques makes use of dry-coupling transducers that have an elastomer face layer [6], [7]. Techniques using air-coupled transducers are possible for the transduction of ultrasound in air so long as frequencies of some megahertz are used [8]–[10]. Alternatively, ultrasound in air can be generated by a laser pulse [11] and the Lorentz force [12]. However, the high frequency ultrasound required for performing high-resolution imaging is not yet available for the aforementioned techniques.

In contrast with these techniques, the dry-contact technique, which transmits the ultrasound through a thin, solid layer inserted between the coupling liquid and the tested parts, uses the coupling liquid. But the tested parts are prevented from being wet with the coupling liquid by the layer [13]–[15]. Drinkwater *et al.* [16] have reported the pressure required for achieving the perfect acoustic coupling at the interface between a typical soft rubber layer and the tested parts with roughened surfaces. We also have shown that the high-frequency ultrasound is capable of transmitting through the interface between a thin, solid layer and the tested parts with an applied pressure of about 0.1 MPa, and realized the acoustic imaging of an interface in semiconductor devices under a dry-contact condition [15].

This paper describes more effective transmission and reception of higher frequency ultrasound through a thin, solid layer, which over the usual water immersion case in points of the spatial resolution and the SNR. By designing the layer based on the theoretical model described in this paper, which calculates the change in the amplitude spectrum with inserting the layer, two frequency operations for getting the higher quality acoustic images than the usual immersion case are realized. One is the signal amplification for the SNR enhancement. Another is the signal modulation toward the higher frequency components for improving the spatial resolution. In practice, we carry out the ultrasonic transmission into silicon through the layers made of polyvinylidene chloride (PVDC) and polyvinyl chloride (PVC), and realize these frequency operations. Also, the present dry-contact technique is applied to the solder joint inspection of a wafer level package. The present dry-contact technique realizes the higher spatial resolution and the higher SNR over the usual water immersion technique without getting the package wet, and clearly shows the defective joint.

Manuscript received April 3, 2003; accepted December 6, 2003. This work was partly supported by the Ministry of Education, Culture, Sports, Science and Technology of Japan under Grant-in-Aid for JSPS Fellows 07019 and Grant-in-Aid for Specially Promoted Research (COE)(2) 11CE2003 and the Mitutoyo Association for Science and Technology under Grant No. R0204.

The authors are with the Department of Mechanical Engineering, Tohoku University, Aoba 01, Aramaki, Aoba-ku, Sendai 980-8579, Japan (e-mail: tohmyoh@ism.mech.tohoku.ac.jp).

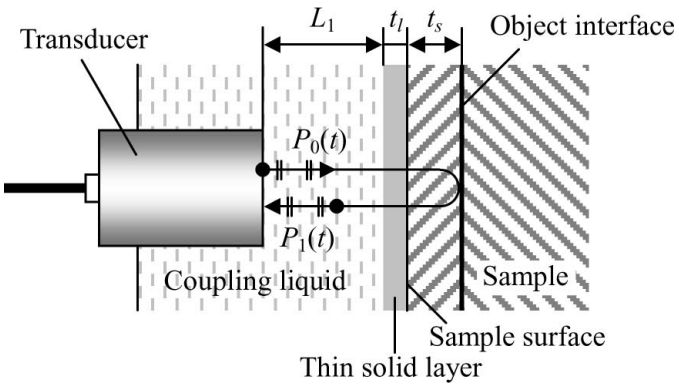

Fig. 1. Schematic of the ultrasonic transmission model through a thin, solid layer.

II. Theory of Ultrasonic Transmission Through a Thin, Solid Layer

A theoretical model of the ultrasonic transmission through a thin, solid layer is developed to design the layer that would perform the effective transduction of high-frequency ultrasound. A schematic of the transmission model is shown in Fig. 1. The plane wave emitted by a transducer reaches an object interface in the sample at normal incidence, and the reflected wave returns to the transducer. A thin, solid layer is now inserted between the coupling liquid and the sample such that the layer is adjacent to the sample surface. It is assumed that the distance traveled between the sample surface and the object interface, t_s, is much larger than the layer thickness, t_l, and the object interface in the sample is composed of two media with sufficient thickness. If the displacement continuity between the layer and the sample surface is maintained during ultrasonic transmission, the Fourier transform, Φ_1, of the echo from the object interface can be expressed as:

$$\begin{aligned}\Phi_1(\nu) &= \int_{-\infty}^{+\infty} P_1 \exp(-i\nu t)dt \\ &= \int_{-\infty}^{+\infty} P_0\alpha_1 T_1 RD \exp(-i\nu t)dt,\end{aligned} \tag{1}$$

where ν is the ultrasound frequency, t is time, P_1 and P_0 are the acoustic pressure of the reflected and emitted waves, i is $\sqrt{-1}$, R is the reflection coefficient at the object interface, and D is a term representing the diffraction effect. The values of α_1 and T_1 are given by:

$$\alpha_1(\nu) = \exp[-2(\alpha_s t_s + \alpha_l t_l + \alpha_c L_1)], \tag{2}$$

and [17]:

$$T_1(\nu) = \frac{4Z_cZ_s/(Z_c+Z_s)^2}{\left[\cos k_l t_l + i\dfrac{Z_cZ_s + Z_l^2}{(Z_c+Z_s)\,Z_l}\sin k_l t_l\right]^2}, \tag{3}$$

where α_s, α_l, and α_c are the ultrasonic attenuation coefficients of the sample, the layer, and the coupling liquid, L_1 is the distance between the transducer and the layer, ρ_c, c_c, and $Z_c[=\rho_c c_c]$ are the density, the ultrasonic velocity, and the acoustic impedance of the coupling liquid, respectively, ρ_s, c_s, and $Z_s[=\rho_s c_s]$, and ρ_l, c_l, and $Z_l[=\rho_l c_l]$ are the equivalent symbols for the sample and the layer, and $k_l[=2\pi\nu/c_l]$ is the ultrasonic wave number in the layer. In the case without the layer, however, the Fourier transform of the echo from the object interface is given by:

$$\begin{aligned}\Phi_2(\nu) &= \int_{-\infty}^{+\infty} P_2 \exp(-i\nu t)dt \\ &= \int_{-\infty}^{+\infty} P_0\alpha_2 T_2 RD \exp(i\nu t)dt,\end{aligned} \tag{4}$$

where:

$$\alpha_2(\nu) = \exp[-2(\alpha_s t_s + \alpha_c L_2)], \tag{5}$$

$$T_2 = 4Z_cZ_s/(Z_c+Z_s)^2, \tag{6}$$

and L_2 is the distance between the transducer and the sample surface. Here, L_1 can be assumed to be the same as L_2 because the layer is very thin. Therefore, the decibel representation of the amplitude ratio is given by:

$$N(\nu, t_l, \zeta) = 20\log\left(\frac{\phi_1}{\phi_2}\right) = 20\log n, \tag{7}$$

where:

$$n(\nu, t_l, \zeta) = \frac{\cos(-2\alpha_l t_l)}{\cos^2 k_l t_l + \dfrac{(\zeta Z_c^2 + Z_l^2)^2}{(1+\zeta)^2 Z_c^2 Z_l^2}\sin^2 k_l t_l}, \tag{8}$$

$$\zeta = Z_s/Z_c, \tag{9}$$

and $\phi_1[=|\Phi_1|]$ and $\phi_2[=|\Phi_2|]$ are the amplitude spectra of Φ_1 and Φ_2, respectively.

TABLE I
Acoustic Properties of Used, Thin, Solid Layers. Frequency ν is in Megahertz.

Layer	Acoustic impedance ($\mathrm{MNm^{-3}s}$)	Density ($\mathrm{kg/m^3}$)	Ultrasonic velocity (m/s)	Attenuation coefficient (1/mm)
PVDC	3.232	1646	1964	$0.0058\nu^2 + 0.1628\nu$
PVC	2.524	1123	2248	$0.0063\nu^2 - 0.0652\nu$

III. Verification of Transmission Model

A. Calculation of Amplitude Ratio

The acoustic properties of the thin, solid layers used in this study, which were made of PVDC and PVC, are summarized in Table I. The acoustic impedance was measured by the method proposed by Kumar *et al.* [18], and the ultrasonic velocity was determined by dividing the acoustic impedance by the measured density. Also, the attenuation coefficient was measured by the method described in [15].

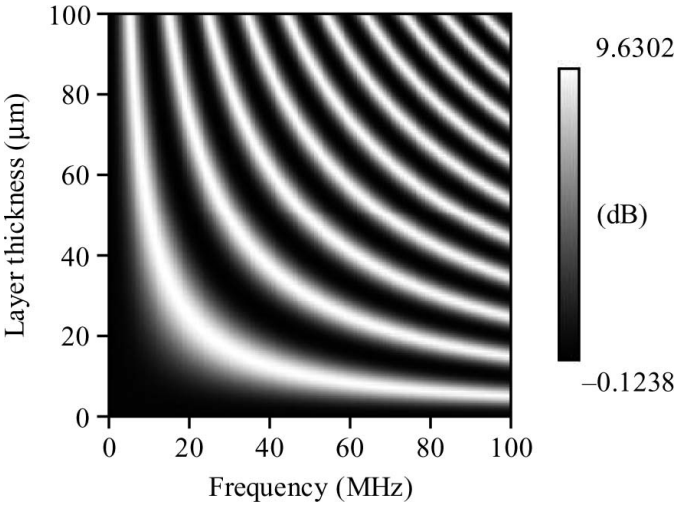

Fig. 2. Amplitude ratio calculated on the transmission system from water to silicon through the PVDC layer as a function of frequency and the layer thickness.

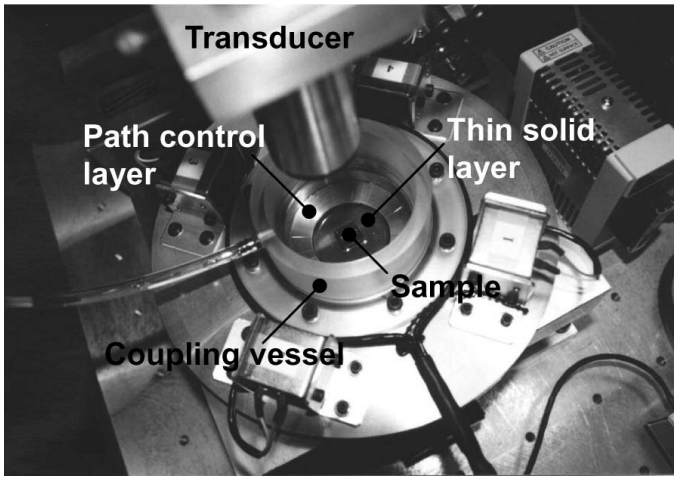

Fig. 3. Details of the dry-contact unit used for keeping the displacement continuity between the thin solid layer and the sample surface during ultrasonic transmission.

The attenuation coefficient of PVDC is always larger than that of PVC for a frequency ν.

The amplitude ratio of the transmission system from water as the usual coupling liquid to silicon via the PVDC layer, which was calculated from (7), (8), and (9), is plotted as a function of frequency and the layer thickness in Fig. 2. The data used in this calculation were the acoustic impedance $Z_c = 1.506$ MNm^{-3}s and $Z_s = 21.832$ MNm^{-3}s [3]. Fig. 2 shows that the peak frequencies in which the amplitude ratio takes the extreme values exist for a layer thickness. This is due to a resonance phenomenon of acoustic wave among water, the layer and silicon, and the layer acts as an acoustic matching layer between water and silicon. Let us denote the lowest peak frequency of the amplitude ratio for a layer thickness by $\nu_{p1,N}$.

By selecting the layer thickness based on the calculated amplitude ratio, two frequency operations for acquiring the high-quality acoustic images will be achieved. One is the signal amplification expressed as:

$$N(\nu) > 0 \text{ dB}. \tag{10}$$

If we select the layer thickness as the peak frequency of the observed echo is coincident with that of the amplitude ratio, the echo will be amplified effectively and the SNR will remarkably be enhanced. However, if we select the layer thickness as the peak frequency of the observed echo is less than that of the amplitude ratio, the higher frequency components of the observed echo preferentially will be amplified and the echo will be modulated toward the higher frequency components. Namely, the value of the signal modulation is described by:

$$\Delta\nu_p = \nu_{p,1} - \nu_{p,2} > 0, \tag{11}$$

where $\nu_{p,1}$ and $\nu_{p,2}$ are the peak frequencies of ϕ_1 and ϕ_2, respectively. The signal modulation toward the higher frequency components is effective for improving the spatial resolution.

B. Realization of Two Frequency Operations

The sample used to confirm the realization of two frequency operations was a disk of 25-mm diameter and 2.1-mm thick, in which a silicon chip $4.67 \times 3.52 \times 0.6$ mm was embedded in the epoxy resin. The ultrasound was transmitted from the side with a bare silicon chip, and the echoes from the silicon/epoxy resin interface were recorded by the present dry-contact technique using the PVDC and PVC layers and the usual water immersion technique. The surface roughness of the sample is expressed by two parameters which are β describing the height of the roughness and γ describing its distribution, and it affects the signal loss at the layer/sample interface. Drinkwater *et al.* [16] suggested that the signal loss at the rubber/solid interfaces is decreased with decreasing β if γ is constant, and the signal loss decreased with increasing γ if β is constant. In this paper, the arithmetical mean deviation of the profile and the profile element width measured by a surface roughness measuring instrument are shown as the typical values of β and γ, respectively. The values of β and γ of the silicon chip were 0.09 μm and 5 μm, respectively. We have reported that the used thin, solid layers achieve good acoustic coupling with the sample under the applied pressure of about 0.1 MPa, and the acoustic coupling of these layers with the sample having such surface roughness is over 90% as compared with the perfect acoustic coupling without coupling loss at the layer/sample interface [15].

Fig. 3 shows the dry-contact unit used for keeping the displacement continuity between the layer and the sample surface during ultrasonic transmission. By evacuating the air between the layer and the sample through the path control layer connected to the vacuum pump having the ultimate pressure of 7 kPa, the pressure of about 0.1 MPa works on the layer/sample interface [19].

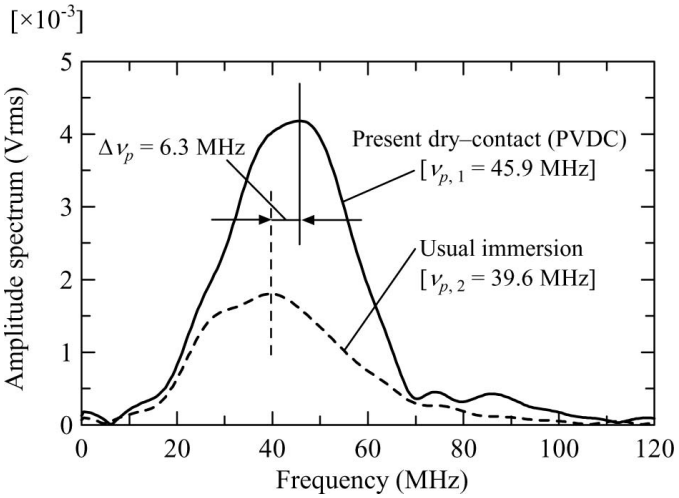

Fig. 4. Examples of the amplitude spectra of the echoes from the silicon/epoxy resin interface obtained by the 50 MHz transducer.

The transducers with nominal frequencies of 30, 50, and 100 MHz and the diameter of the piezoelectric element of 6.35 mm (Panametrics, Waltham, MA) were used. The transducer with 30 MHz nominal frequency had a focal length of 19.05 mm, and the length of 50 and 100 MHz transducers was 12.7 mm.

The values of $\nu_{p,2}$ of the echoes from the silicon/epoxy resin interface obtained by the 30, 50, and 100 MHz transducers were 25.4, 39.6, and 65.4 MHz, respectively. To effectively amplify the echo of the 100 MHz transducer, the PVDC and PVC layers of 9-μm thick were used. The values of $\nu_{p1,N}$ of the PVDC and PVC layers of 9-μm thick were 54.7 and 62.5 MHz, and those were near to the value of $\nu_{p,2}$ of the 100 MHz transducer. Those layers also were used for effectively modulating the echoes of the 30 and 50 MHz transducers toward the higher frequency components. Examples of the amplitude spectra of the echoes from the silicon/epoxy resin interface obtained by the 50 MHz transducer, which were obtained by the present dry-contact technique using the PVDC layer and the usual immersion technique, are shown in Fig. 4. Fig. 4 clearly shows that the signal amplification in the frequency range of 20 to 60 MHz and the signal modulation toward the higher frequency components are realized through the PVDC layer of 9-μm thick. The comparison between the theoretical amplitude ratio and the experimental one in the cases of the PVDC and PVC layers is shown in Figs. 5(a) and (b), respectively. Also, the values of $\Delta\nu_p$ in the cases of the 30, 50, and 100 MHz transducers are shown in Fig. 5. The theoretical amplitude ratio gives reasonable agreement with the experimental one for both layers. In the case of the 100 MHz transducer, the echoes were not effectively modulated for both layers, but those were remarkably amplified as compared with the usual water immersion case. However, in the cases of the 30 and 50 MHz transducers, the signal modulation toward the higher frequency components are realized for both layers at the expense of the signal amplification. In comparison

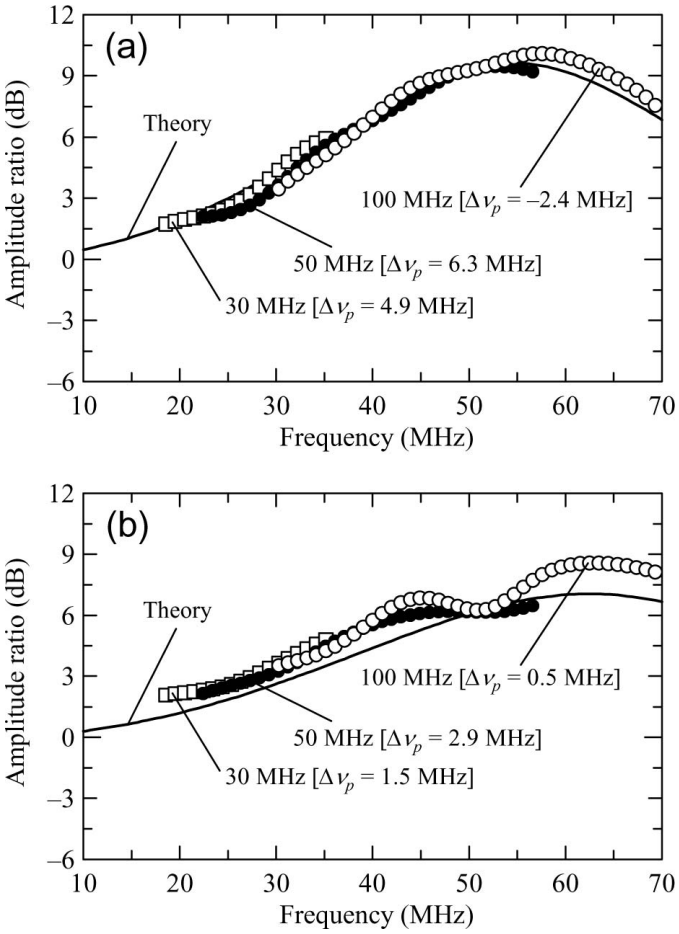

Fig. 5. Comparison between the theoretical amplitude ratio and the experimental one in the cases of the 30, 50, and 100 MHz transducers. The values of the signal modulation are shown as $\Delta\nu_p$. (a) PVDC layer and (b) PVC layer.

with the PVDC and PVC layers, the echoes obtained by the 30 and 50 MHz transducers through the PVDC layer were modulated toward the higher frequency components than those of the PVC layer. This fact suggests that the layer having the steeper slope of the amplitude ratio curve in the frequency range of the observed echo gives effective modulation.

IV. Application to Solder Joint Inspection

A. Acoustic Imaging

The examined package was a wafer-level package with a bare silicon chip having β of 0.08 μm and γ of 3 μm, and it was already mounted on the printed circuit board by a ball-grid array assembly as shown in Fig. 6(a). Fig. 6(b) shows the back-wall view of the package before mounting. The diameter of the balls and the terminal pitch were 0.35 and 0.50 mm, respectively. An arrow in Fig. 6(b) indicates the defective joint introduced by the hot bump pull testing, and the solder ball was pulled out from the pad/solder ball interface. The acoustic imaging of the jointing interface

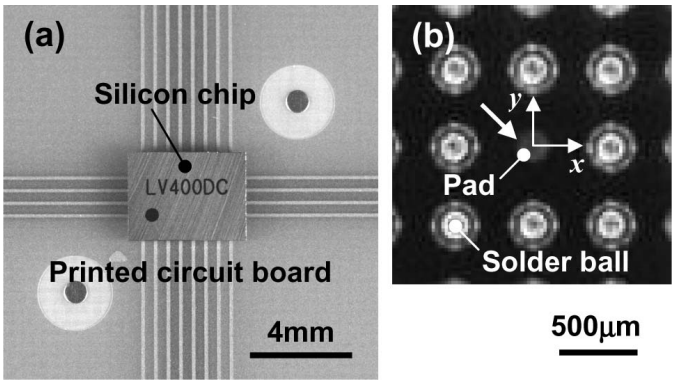

Fig. 6. Examined wafer level package. (a) Whole view of the package mounted on the printed circuit board. (b) Back-wall view of the package before mounting. The defective joint is indicated by an oblique arrow.

was carried out by the present dry-contact technique using the PVDC and PVC layers and the usual water immersion technique. The used transducers were the 50 and 100 MHz transducers, and the scan pitch was 0.012 mm.

The echo amplitude distributions in the y-direction at $x = 0$ measured by the present dry-contact technique using the PVDC layer and the usual immersion technique are shown in Fig. 7. The distributions in the cases of the 50 and 100 MHz transducers are shown in Figs. 7(a) and (b), respectively, and the defective joint is indicated by an arrow in Fig. 7. Fig. 7(a) shows that the defective joint is clearly discriminated from the sound joints by the present dry-contact technique using the PVDC layer. However, in spite of using the same 50 MHz transducer, the detection of the defective joint is difficult for the usual immersion technique because the values of echo amplitude in the defective and sound joints are almost the same. However, in the case of the 100 MHz transducer shown in Fig. 7(b), the defective joint can clearly be detected by both techniques. The acoustic images of the jointing interface beneath the silicon chip obtained by the 100 MHz transducer are shown in Fig. 8. In both images obtained by the present dry-contact technique using the PVDC layer [Fig. 8(a)] and the usual immersion technique [Fig. 8(b)], the defective joint is clearly visualized.

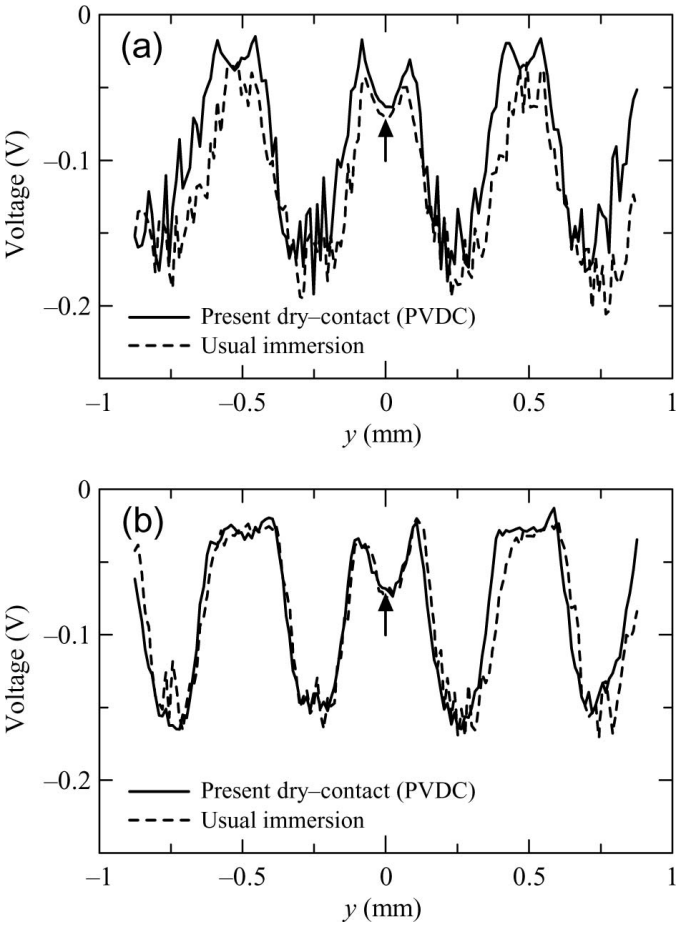

Fig. 7. Echo amplitude distributions in the y-direction at $x = 0$. (a) 50 MHz transducer and (b) 100 MHz transducer. The defective joint is indicated by an arrow.

B. Quality of Acoustic Images

The decibel representation of the detectability of the defective joint is expressed as:

$$\Lambda = 20 \log \left(\frac{P^d}{P^s} \right), \tag{12}$$

where P^d and P^s are the average echo amplitude in the defective and sound joints, respectively, and the defective joint can be found out provided that the detectability of the defective joint is over 0 dB. Comparison of the detectability of the defective joint between the present dry-contact and the usual immersion techniques is shown in Fig. 9. In the case of the 50 MHz transducer, the de-

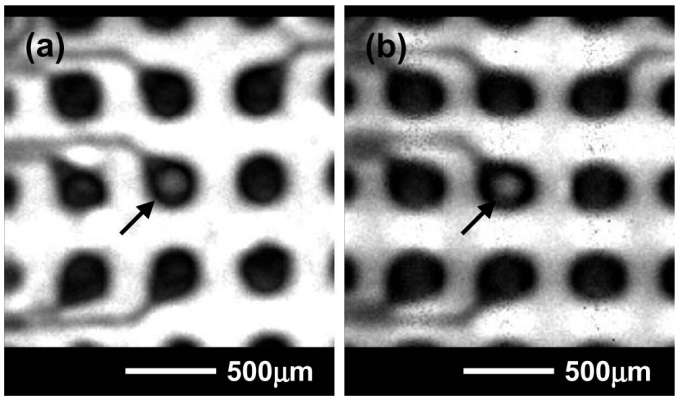

Fig. 8. Acoustic images of the jointing interface beneath the silicon chip obtained by the 100 MHz transducer. (a) Present dry-contact technique using the PVDC layer. (b) Usual immersion technique. The defective joint is indicated by an arrow.

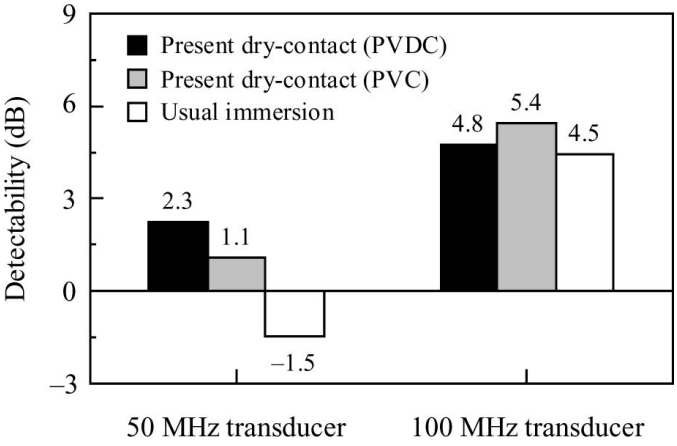

Fig. 9. Comparison of the detectability of the defective joint between the present dry-contact and the usual immersion techniques.

TABLE II
ESTIMATED LATERAL RESOLUTION, d^{PE}, AND THE SNR IN THE DEFECTIVE JOINT.

	Nominal transducer frequency (MHz)			
	50		100	
Technique	d^{PE} (μm)	SNR (dB)	d^{PE} (μm)	SNR (dB)
Present (PVDC)	70	26.9	47	29.3
Present (PVC)	72	28.1	46	24.6
Usual immersion	88	25.0	47	22.7

tectability of the defective joint was remarkably improved by the present dry-contact technique as compared with the usual immersion technique, especially in the case of the PVDC layer. However, the detectability of the defective joint of the present dry-contact and the usual immersion techniques was almost the same for the 100 MHz transducer.

The estimated lateral resolution, d^{PE}, and the SNR in the defective joint are summarized in Table II. The values of d^{PE} were estimated by the effective point-spread function determined from the amplitude spectra of the backwall echoes of the package [1], [20]. Also, the SNR in the defective joint was determined by the following equation:

$$SNR = 10\log\left[\sum_{i=1}^{Y_s}\left(\frac{E_s^2}{Y_s}\right)\Big/\sum_{i=1}^{Y_n}\left(\frac{E_n^2}{Y_n}\right)\right], \quad (13)$$

where E_s and E_n are the echo signal from the defective joint and the noise signal, and Y_s and Y_n are the length of E_s and E_n, respectively. The signal E_n was measured from the nonsignal interval recorded with E_s. Table II shows that the values of d^{PE} are remarkably improved by the present dry-contact technique as compared with the usual immersion technique in the case of the 50 MHz transducer. This was due to the preferential amplification of the higher frequency components of the emitted wave, and the improvement of the detectability of the defective joint shown in Fig. 9 is interpreted as the improvement of spatial resolution brought by the signal modulation toward the higher frequency components. But, in the case of the 100 MHz transducer, because the higher and lower frequency components of the emitted wave were equivalently amplified through those layers, the values of d^{PE} and the detectability of the defective joint were almost the same for both techniques. However, especially in the case of using the PVDC layer, because the emitted wave was effectively amplified, the SNR was remarkably enhanced by the present dry-contact technique as compared with the usual immersion technique. Therefore, the higher quality acoustic image that indicated lower noise over the usual immersion image [Fig. 8(b)] was acquired by the present dry-contact technique using the PVDC layer as shown in Fig. 8(a).

V. Conclusions

We have presented the theoretical model to design a thin, solid layer that produces the high-quality acoustic image of an object interface in the sample without getting the sample wet. By inserting the layer designed from the model between the coupling liquid and the sample, two frequency operations—which are the signal amplification for the SNR enhancement and the signal modulation toward the higher frequency components for improving the spatial resolution—are realized. We also performed the ultrasonic transmission from water to silicon through the layers made of PVDC and PVC, and demonstrated two frequency operations through the interfaces between those layers and silicon with an applied pressure of about 0.1 MPa. In practice, we carried out the solder joint inspection of a wafer-level package. In the case of using the 50 MHz transducer, it was difficult to discriminate the defective joint from the sound joints for the usual water immersion technique, but the present dry-contact technique clearly detected the defective joint by improving the spatial resolution. Also, the SNR in the case of using the 100 MHz transducer was remarkably enhanced by the present dry-contact technique as compared with the usual water immersion technique.

References

[1] S. Canumalla, "Resolution of broadband transducers in acoustic microscopy of encapsulated ICs: Transducer selection," *IEEE Trans. Comp. Packag. Technol.*, vol. 22, no. 4, pp. 582–592, 1999.

[2] A. J. Rogovsky, "Development and application of ultrasonic dry-contact and air-contact C-scan systems for nondestructive evaluation of aerospace composites," *Mater. Eval.*, vol. 49, no. 12, pp. 1491–1497, 1991.

[3] R. S. Gilmore, "Industrial ultrasonic imaging and microscopy," *J. Phys. D: Appl. Phys.*, vol. 29, no. 6, pp. 1389–1417, 1996.

[4] A. A. O. Tay, G. L. Tan, and T. B. Lim, "Predicting delamination in plastic IC packages and determining suitable mold compound properties," *IEEE Trans. Comp., Packag., Manufact. Technol. B*, vol. 17, no. 2, pp. 201–208, 1994.

[5] K. Liao and Y.-M. Tan, "Influence of moisture-induced stress on in situ fiber strength degradation of unidirectional polymer composite," *Composites Part B*, vol. 32, no. 4, pp. 365–370, 2001.
[6] A. M. Robinson, B. W. Drinkwater, and J. Allin, "Dry-coupled low frequency ultrasonic wheel probes: Application to adhesive bond inspection," *NDT & E Int.*, vol. 36, no. 1, pp. 27–36, 2003.
[7] K.-H. Im, D. K. Hsu, and H. Jeong, "Material property variations and defects of carbon/carbon brake disks monitored by ultrasonic methods," *Composites Part B*, vol. 31, no. 8, pp. 707–713, 2000.
[8] D. W. Schindel, D. A. Hutchins, L. Zou, and M. Sayer, "The design and characterization of micromachined air-coupled capacitance transducers," *IEEE Trans. Ultrason., Ferroelect., Freq. Contr.*, vol. 42, no. 1, pp. 42–50, 1995.
[9] I. Ladabaum, B. T. Khuri-Yakub, and D. Spoliansky, "Micromachined ultrasonic transducers: 11.4 MHz transmission in air and more," *Appl. Phys. Lett.*, vol. 68, no. 1, pp. 7–9, 1996.
[10] B. Hosten, D. A. Hutchins, and D. W. Schindel, "Measurement of elastic constants in composite materials using air-coupled ultrasonic bulk waves," *J. Acoust. Soc. Amer.*, vol. 99, no. 4, pp. 2116–2123, 1996.
[11] D. K. L. Don-Liyanage and D. C. Emmony, "Schlieren imaging of laser-generated ultrasound," *Appl. Phys. Lett.*, vol. 79, no. 20, pp. 3356–3357, 2001.
[12] H. Ogi, M. Hirao, and K. Minoura, "Noncontact measurement of ultrasonic attenuation during rotating fatigue test of steel," *J. Appl. Phys.*, vol. 81, no. 8, pp. 3677–3684, 1997.
[13] C. J. Brotherhood, B. W. Drinkwater, and F. J. Guild, "The effect of compressive loading on the ultrasonic detectability of kissing bonds in adhesive joints," *J. Nondestr. Eval.*, vol. 21, no. 3, pp. 95–104, 2002.
[14] H. Tohmyoh and M. Saka, "Development of a dry-contact ultrasonic technique and its application to NDE of IC packages," in *Recent Advances in Experimental Mechanics*. E. E. Gdoutos, Ed. Dordrecht: Kluwer Academic, 2002, pp. 443–454.
[15] H. Tohmyoh and M. Saka, "Dry-contact technique for high-resolution ultrasonic imaging," *IEEE Trans. Ultrason., Ferroelect., Freq. Contr.*, vol. 50, no. 6, pp. 661–667, 2003.
[16] B. Drinkwater, R. Dwyer-Joyce, and P. Cawley, "A study of the transmission of ultrasound across solid-rubber interfaces," *J. Acoust. Soc. Amer.*, vol. 101, no. 2, pp. 970–981, 1997.
[17] L. E. Kinsler, A. R. Frey, A. B. Coppens, and J. V. Sanders, "Transmission phenomena," in *Fundamentals of Acoustics*. 3rd ed. New York: Wiley, 1982, pp. 127–131.
[18] A. Kumar, B. Kumar, and Y. Kumar, "A novel method to determine the acoustic impedance of membrane material," *Ultrasonics*, vol. 35, no. 1, pp. 53–56, 1997.
[19] H. Tohmyoh and M. Saka, "A dry-contact method for transmitting higher frequency components of ultrasound," *Int. J. Appl. Electromag. Mech.*, vol. 18, no. 1-3, pp. 31–39, 2003.
[20] L. Bechou, Y. Ousten, B. Tregon, F. Marc, Y. Danto, R. Even, and P. Kertesz, "Ultrasonic images interpretation improvement for microassembling technologies characterization," *Microelectron. Reliab.*, vol. 37, no. 10/11, pp. 1787–1790, 1997.

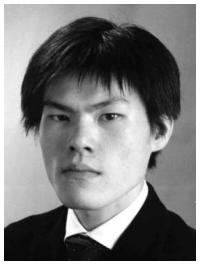

Hironori Tohmyoh received the B.Sc. and M.Sc. degrees in mechanical engineering from the University of Electro-Communications, Tokyo, Japan, in 1998 and 2000, respectively. He received the Ph.D. degree in mechanical engineering in 2003 from Tohoku University, Sendai, Japan.

He is currently a research fellow of the Japan Society for the Promotion of Science. His research interest is the application of dry-contact ultrasonic technique to the evaluation of material.

Masumi Saka received the B.Eng. degree in mechanical engineering in 1977 and the Dr.Eng. degree in mechanical engineering in 1982, both from Tohoku University, Sendai, Japan. He became a professor at Tohoku University in 1993.

Dr. Saka received the JSME Medals in 1992 and 2000, the Best Paper Awards from the Japanese Society for Non-Destructive Inspection in 1991 and 2002, the R. E. Peterson Award in 1992 from the Society for Experimental Mechanics, and some other awards on Sensing and Evaluation of Materials System.